Easterly wave contributions to seasonal rainfall over the tropical Americas in observations and a regional climate model

Christian Dominguez[1] · James M. Done[2] · Cindy L. Bruyère[2,3]

Abstract

Easterly waves (EWs) are important moisture carriers and their variability can impact the total May–November rainfall, defined as seasonal precipitation, over the Tropical Americas. The contribution of EWs to the seasonal precipitation is explored over the tropical Americas using rain gauge stations, reanalysis data and a regional model ensemble during the 1980–2013 period. In the present study, EWs are found to produce up to 50% of seasonal rainfall mainly over the north of South America and contribute substantially to interannual regional rainfall variability. An observational analysis shows that the El Niño Southern Oscillation (ENSO) affects EW frequency and therefore, their contribution to seasonal rainfall. In recent years, tropical cyclone (TC) activity over the Main Development Region (MDR) of the tropical North Atlantic has a negative impact on regional seasonal precipitation over northern South America. High TC activity over MDR corresponds to below-normal precipitation because it reduces the EW activity reaching northern South America through the recurving of TC tracks. Recurving TC tracks redirect moisture away from the tropical belt and into the mid-latitudes. However, this relationship only holds under neutral ENSO conditions and the positive phase of the Atlantic Multidecadal Oscillation. A 10-member regional model multi-physics ensemble simulation for the period 1990–2000 was analyzed to show the relationships are robust to different representations of physical processes. This new understanding of seasonal rainfall over the tropical Americas may support improved regional seasonal and climate outlooks.

Keywords Easterly waves · Seasonal precipitation · Tropical cyclone tracks · Observations · Regional model

1 Introduction

Convectively coupled equatorial waves (CCEWs) are responsible for transporting moisture, momentum, and heat over the tropics and producing up to 20% of the tropical intraseasonal precipitation variance (Lubis and Jacobi 2015). They also play a dominant role in influencing tropical

✉ Christian Dominguez
dosach@atmosfera.unam.mx

1. Centro de Ciencias de la Atmósfera, Universidad Nacional Autónoma de México (UNAM), Circuito Exterior, Ciudad Universitaria, 04510 Mexico City, Mexico

2. National Center for Atmospheric Research, Boulder, CO, USA

3. Environmental Sciences and Management, North-West University, Potchefstroom, South Africa

climate because their seasonal and interannual variability drives changes in tropical rainfall. Easterly Waves (EWs) are CCEWs that travel westwards, and their structure is Rossby wave-like. EWs produce significant amounts of rainfall in the tropics that affect large populations over this region. This type of CCEW is also well-known as a precursor of tropical cyclones (TCs) particularly over the North Atlantic and Eastern Pacific Oceans (Pasch et al. 1998; Schreck et al. 2012).

Some studies (Walter et al. 2003; Kiladis et al. 2009; Crétat et al. 2015) describe EWs, commonly called tropical depression type waves, as synoptic waves that have well-organized cumulus, periods of 2–6 days, group speed of 5–10 m/s and favor the occurrence of intense precipitation in places such as West Africa. EWs occur from May to November and carry moisture from oceans to land (Thorncroft and Hodges 2001), mainly during September and October when they are more active (Jiang and Zipser 2010). However, most investigations have focused on understanding connections between EWs and daily rainfall over African regions, for instance the Sahel region, rather than other regions such as

the Tropical Americas (TAs) and its adjacent continental landmass (Fig. 1). Understanding the role of EW activity for continental and seasonal rainfall over TAs may support socioeconomic planning of activities dependent on regional, seasonal water availability.

Tropical cyclones (TCs) are also important moisture carriers. Arid or semi-arid regions can benefit greatly from a single TC event because one system can produce such intense precipitation (Dominguez and Magaña 2018). TCs are well known for transporting moisture from the tropics to the subtropics and mid-latitudes, but they also can induce drying conditions in regions that are remote to their circulation, approximately more than 500 km (Dominguez and Magaña 2018). This drying effect has been rarely explored and quantified. It is explained in terms of weak subsidence outside the core of the system that is forced mechanically and may produce clear skies and moisture divergence in neighboring regions to the TC system (Emanuel 1997; Dominguez and Magaña 2018). In other words, while some arid or semi-arid regions are favored by TC occurrence, other distant regions from the TC center can be adversely affected in their accumulated seasonal rainfall. For example, Marengo et al. (2008) explored the causes and effects of droughts over northern South America, mainly over the Amazonian region, that occurred during 2005. In this year, the North Atlantic TC activity was very high. This study showed that a weakened easterly flow and reduced upward motion resulted in a decrease of rainfall and consequently, a severe drought.

El Niño Southern Oscillation (ENSO) dominates precipitation patterns in the tropics and subtropics on 2 to 7-year timescales. Under La Niña conditions, extreme rainfall events are more likely to occur because subsidence decreases over southern Mexico and the Caribbean Region (Magaña et al. 2003). This allows tropical convection to develop over those regions, and the Hadley circulation also strengthens the convection produced by its upward air motion over northern South America (Wang and Enfield 2003; Arias et al. 2015). On the other hand, under El Niño conditions, deep convection can be inhibited leading to negative precipitation anomalies over those regions (Wang and Enfield 2003) because of strong induced subsidence (Magaña et al. 2003). Summer seasons under neutral ENSO conditions do not show a clear signal in seasonal precipitation, since no strong seasonal dynamical teleconnections exist, resulting in low seasonal predictability (Barnston et al. 2010). In the absence of strong dynamical ENSO forcing, other processes such as the continuation of long-term trends, persistence of anomalies, or other subseasonal oscillations such as the Madden–Julian Oscillation (Vitart 2017) can become important. Moreover, longer-term oscillations, such as the Atlantic Multidecadal Oscillation (AMO), have also shown

Fig. 1 Regional climate model domain, showing terrain height (m) and the three study regions: main development region (MDR), northern South America (NSA) and the Tropical Americas (TAs)
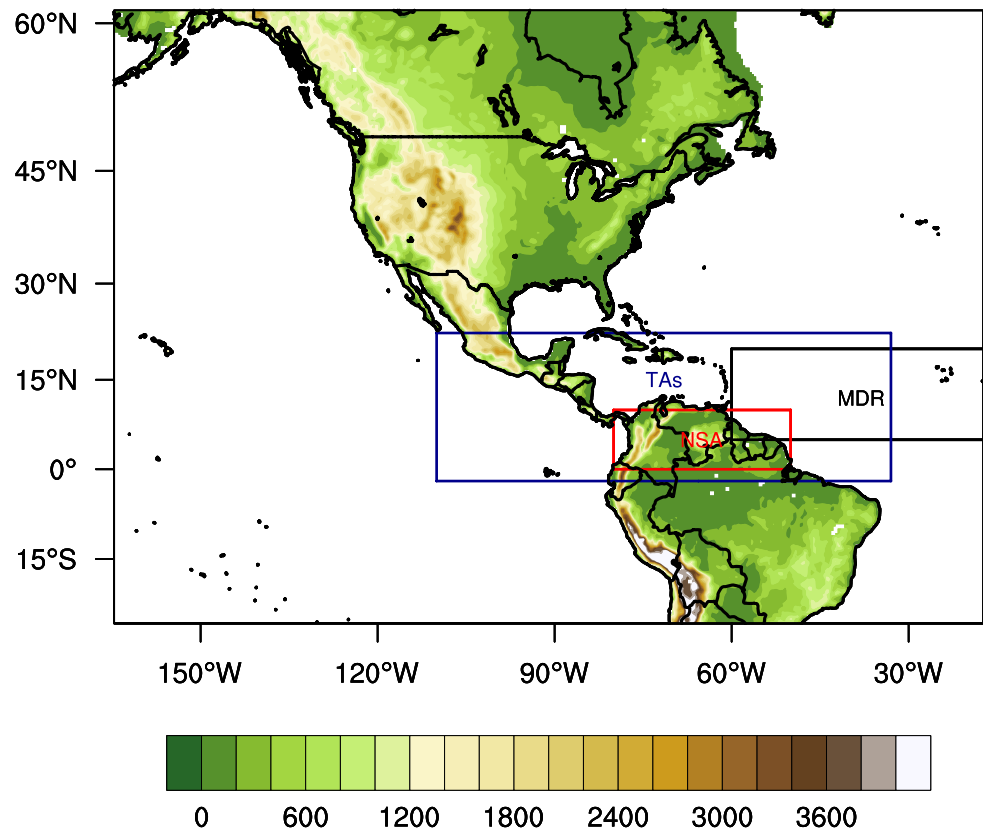
to play a significant role in TC activity over the Atlantic basin, since higher SSTs lead to more TCs and lower SSTs lead to fewer TCs. For instance, Caron et al. (2015) found that under favorable conditions for TC formation, which are present during the positive phase of AMO (AMO+), more EWs become TCs in the Main Development Region (MDR). Their study analyzed maritime rainfall and found a negative relationship between more TCs over the mid-Atlantic Ocean and precipitation off the coast of South America during AMO+.

Previous regional studies of TAs rainfall (Cerveny and Newman 2000; Jiang and Zipser 2010) mostly focus on exploring the footprint of TCs in rainfall and show that TCs contribute up to 20% of seasonal precipitation over this region. These studies suggest that other tropical phenomena could play a larger role in the regional rainfall. For instance, CCEWs, mainly EWs, commonly affect northern South America (NSA), but their impact on regional precipitation has been barely quantified. Here, we build on these studies by exploring dynamical mechanisms that associate EW activity, TC tracks, and regional rainfall to determine their role in regional summer rainfall variability, mainly over NSA (Fig. 1). We hypothesize that high TC activity over the MDR, produce more TCs developing from EWs, and transport moisture into the subtropics, leading to dry summer seasons over the TAs by means of the TC drying effect and few EWs reaching the continental NSA. TCs act as drying agents for the TAs when they are over the mid-Atlantic Ocean because they transport moisture from the tropics to the subtropics, causing negative anomalies of moisture in this region, mainly over NSA (Dominguez and Magaña 2018), and reducing the chances of rainfall over the TAs continental landmass. In addition, more EWs becoming TCs over the MDR mean that few EWs arrive at the TAs and consequently, this could impact the seasonal precipitation over NSA.

The main objective is to understand the role of EW–TC rainfall relationship in seasonal precipitation over TAs, mainly NSA, and determine if this relationship is modified by ENSO phase. The outcomes of this study could be key in understanding the relationship between EWs and seasonal rainfall in order to support improved regional seasonal forecasts. This study investigates the contribution of EWs to seasonal precipitation over the TAs in observations, reanalysis data, and Regional Climate Model (RCM) outputs. Dynamical downscaling performed using RCMs provides detailed information on tropical phenomena, such as TCs and EWs, and regional precipitation (Crétat et al. 2015; Done et al. 2015). A RCM grid spacing of 36-km has proven to capture adequately tropical synoptic circulations and rainfall (Bruyère et al. 2017). Moreover, EW characteristics (spatial distribution, evolution, generation, organized convection and potential vorticity structure) have been realistically

represented by RCMs (Hsieh and Cook 2007; Berry and Thorncroft 2012; Crosbie and Serra 2014), which suggests that RCMs can be used to analyze EWs and their contribution to tropical precipitation.

Analysis of a multi-physics RCM ensemble simulation complements the observational analysis by exploring the different climate response of each member to the same Surface Sea Temperatures (SSTs). In other words, the robustness of the physical mechanisms to different representations of physical processes will be examined in each ensemble member. Here, we develop an understanding of whether RCMs can capture the EW–TC rainfall relationships seen in observations, using the multi-physics ensemble.

The next section describes the observational and reanalysis data, RCM outputs and the methodology used to define EW tracks. The approach to attribute rainfall to EWs is also presented. Section 3 analyses the contribution of EWs to accumulated seasonal precipitation in observations and reanalysis data. Section 4 analyzes contributions of EWs to rainfall in a RCM ensemble. Finally, the summary and conclusions are given in Sect. 5.

2 Data and methods

2.1 Observations and reanalysis

Daily precipitation data from rain gauge stations and buoys are used to analyze the rainfall produced by EWs in the MDR, tropical Americas and the tropical Eastern Pacific Ocean. The surface station data are obtained from the climate information website of the National Weather Services that are located in the study region. Rain gauge stations that had 34 years of data were selected for this analysis. The TAO/TRITON and PIRATA projects provided the buoy precipitation information over the MDR in the North Atlantic Ocean and over the tropical eastern Pacific Ocean during the 1998–2013 period. We focus on data from May to November (hereafter defined as the summer season) when EWs are active.

The original temporal and spatial resolution of Tropical Rainfall Measure Mission (TRMM) 3B42 is 3-hourly and 0.25° respectively. We compared the European Centre for Medium-Range Weather Forecasts ERA-Interim (ERAI) reanalysis, the Climate Forecast System (CFSR) reanalysis and TRMM 3B42 rainfall dataset with the surface station data during the 1998–2013 period. Thus, an assessment of the Brier Skill Score, Normalized Root Mean Square Error and the cumulative minimum value were conducted to determine the extent to which the datasets capture daily rainfall over tropical North America as described by the surface station data (see Supplementary Material: tables ST1, ST2, and ST3). We find that regional precipitation

from ERAI compared most favorably with surface station data (see supplementary material). Kim and Alexander (2013) pointed out that CFSR has the best performance in representing tropical variability. However, they also found that the ERAI reanalysis represents adequately tropical precipitation variability associated with EWs. Another advantage of using ERAI is the number of years that this database provides for long-term climate studies.

Environmental variables including humidity and wind are used to examine EWs (main variables used for tracking EWs as described later). The ERAI reanalysis data, which is available from 1979 to the present and has a T255 spectral resolution (~ 80 km) on 60 vertical model levels (Dee et al. 2011), provided these atmospheric variables. In addition, the EW contribution to summer rainfall is also estimated using the ERAI precipitation dataset. This information helps to compute precipitation associated with EW tracks over the North Atlantic and Eastern Pacific Ocean.

Both objective and subjective techniques have been used to track EWs (Pasch et al. 1998; Thorncroft and Hodges 2001; Berry et al. 2007; Serra et al. 2010; Agudelo et al. 2011) over the North Atlantic Ocean. However, the resulting tracks are sensitive to the method and no official EW track dataset has been established. Following Thorncroft and Hodges (2001), the TRACK technique is implemented to objectively identify EW tracks over the 1980–2013 period. Winds at 850, 700 and 600 hPa from ERAI are averaged, vorticity is calculated, and filtered to remove mesoscale vorticity features and leave synoptic scales. The criteria, the same as used in previous work (Thorncroft and Hodges, 2001; Serra et al. 2010), to define vorticity centers as EWs are:

1. Westward movement
2. Lifetime of at least 2 days
3. First detected points are over the oceanic domain 5°–20°N
4. Vorticity centers are 2.0×10^{-5} s^{-1} or greater
5. Systems travel at least 1000 km.

Thus, mid-latitude systems and topographically-induced waves are removed. This objective method also tracks TCs. To identify TC tracks, hurricane matching is carried out by following the TC centers defined by the best-track database HURDAT of the National Hurricane Center (Landsea and Franklin 2013), in a grid of 2°×2°. This helps to define which TCs came from EWs and remove the portions of TC tracks from our EW track database.

Agudelo et al. (2011) suggested that a 15°×15° region around the center of the wave can be used to capture the EW features. Thus, a threshold distance of 7.5° from the EW center defined by the TRACK technique is used to define the precipitation produced by EWs. However, this step assumes that precipitation matches with the positive phase of EWs and also that the precipitation is confined within the 15°×15° box.

While EW precipitation does not exclusively occur in the positive phase of the wave, it is far from constant throughout all phases of the wave (Serra et al. 2008). Using satellite-based rainfall estimates and reanalysis data over the Atlantic Ocean, Janiga and Thorncroft (2016) found that rainfall typically maximizes in the wave trough where the air is moist. The ridge is characterized by drier air and shallow convection. But they also find substantial variability about these typical conditions. Our focus on only the positive phase may result in an underestimation of the total EW rainfall because we may miss some rainfall associated with the negative phase. This represents a potential limitation of our approach, as discussed in Sect. 5.

In addition, the AMO monthly index was obtained from the detrended Kaplan SST database version 2 (Enfield et al. 2001). Only the values of AMO index from May to November are considered for this study. The Reynolds optimum interpolated (OIv2) dataset (Reynolds et al. 2007) was also analyzed to explore the AMO influence on tropical SSTs.

2.2 Regional climate model experiment design

Using a regional climate model brings about better-resolved phenomena such as TCs or EWs than in coarse resolution global models. Here, we use an existing RCM dataset described by Bruyère et al. (2017) and summarized here. The Weather Research and Forecasting (WRF; Powers et al. 2017) model was driven by the ERAI reanalysis for the 1990–2000 period. The Reynolds optimum interpolated analysis (Reynolds et al. 2007), which has a weekly temporal resolution and 1.0° spatial resolution, was used to force the RCM ensemble. The experiments were designed at the National Center for Atmospheric Research (NCAR) for a large variety of studies. The domain used for the experiments extends from Canada to Brazil and from Hawaii to the west coast of Africa (Fig. 1). The size of the domain is enough for capturing EWs that enter the eastern boundary and become TCs over the North Atlantic Ocean within the RCM domain (Bruyère et al. 2017). Furthermore, the fact that the domain boundaries are far away from our regions of study, let the regional climate processes evolve freely within the WRF domain and they are not constrained by the boundaries (Done et al. 2015). Three specific regions were considered to explore the EW contribution to seasonal rainfall according to their location and summer precipitation: MDR, NSA and TAs (Fig. 1).

For this study, ten members were chosen from a 24-member model physics ensemble. The members that performed adequately in terms of their simulated TC activity were considered, as described in Bruyère et al. (2017).

The ten members have different physical parameterization schemes: (1) *radiation scheme* (CAM: Collins et al. 2006 and RRTMG: Mlawer et al. 1997); (2) *cumulus convection* (Kain Fritsch: Kain and Fritsch 1990, New Simplified Arakawa-Schubert: Han and Pan 2011, and Tiedtke: Tiedtke 1989); (3) *microphysics* (WRF Single-Moment 6-Class: Hong et al. 2004, and Thompson: Thompson et al. 2004) and (4) *planetary boundary layer* (PBL) (Mellor-Yamada-Janjic: Janjic 1994, and Yonsei University: Hong et al. 2006). The ten members were abbreviated as follows: the first letter indicates the radiation scheme (c for CAM and r for RRTMG), the second letter denotes the cumulus parameterization (k for KF, n for NAS and t for Tiedtke), the third character the microphysics (6 for WSM6C and t for Thompson) and the fourth letter represents the planetary boundary layer scheme (m for MYJ and y for YU). The aforementioned physics combinations are commonly used and well-tested (Bruyère et al. 2017). *The Noah scheme* (Chen and Dudhia 2001) was the only land surface scheme used for the experiments. This focuses our study on the robustness of the physical processes to different representations of atmospheric processes.

Vorticity centers are tracked in the 10-member ensemble using the same technique and aforementioned criteria as for ERA-I data. However, vorticity centers had to be 1.8×10^{-5} s^{-1} or greater. An additional criterion of wind speed at 1000 mb was used (less than 12 m/s for KF simulations and 10 m/s for the rest of the simulations), since TC tracks in the ensemble were defined using these thresholds (Bruyère et al. 2017). In this way, TCs that came from EWs in the outputs were detected and the portion of the tracks that were TCs was removed from the EW track database.

3 Results: easterly wave contributions to seasonal rainfall in observations

3.1 Easterly wave contributions to rainfall over the tropical Americas in the period 1980–2013

The TAs region has different climatic rainfall regimes. While the Caribbean region receives around 600 mm annually, the amount of seasonal precipitation over Panama can be greater than 1000 mm per year (Fig. 2a). As mentioned before, the precipitation produced by EWs is defined as the rainfall that is at a threshold distance of 7.5° from the EW center defined by the TRACK technique, as proposed by Agudelo et al. (2011). Then, the seasonal precipitation attributed to EWs is obtained by adding all the precipitation associated with the EW tracks for each year. The climatological EW precipitation is an average of this seasonal amount for the 1980–2013 period.

EWs can act as moisture carriers that transport humidity from the MDR to the Eastern North Pacific Ocean (ENP). EWs produce up to 400 mm per year over the MDR and at least 600 mm over the ENP (Fig. 2b). Over tropical landmass, Costa Rica and Panama are greatly impacted by EW rainfall, since these regions can receive up to 700 mm per year. However, other mechanisms such as the Caribbean Low-Level Jet (CLLJ) and Chocó Jet can be significant contributors to the seasonal rainfall over these regions (Arias et al. 2015). EW tracks are also important moisture carriers over southern Mexico, the Caribbean region and NSA (Fig. 2b). Here, the interannual variability of EWs may result in wet or dry years, depending on the region.
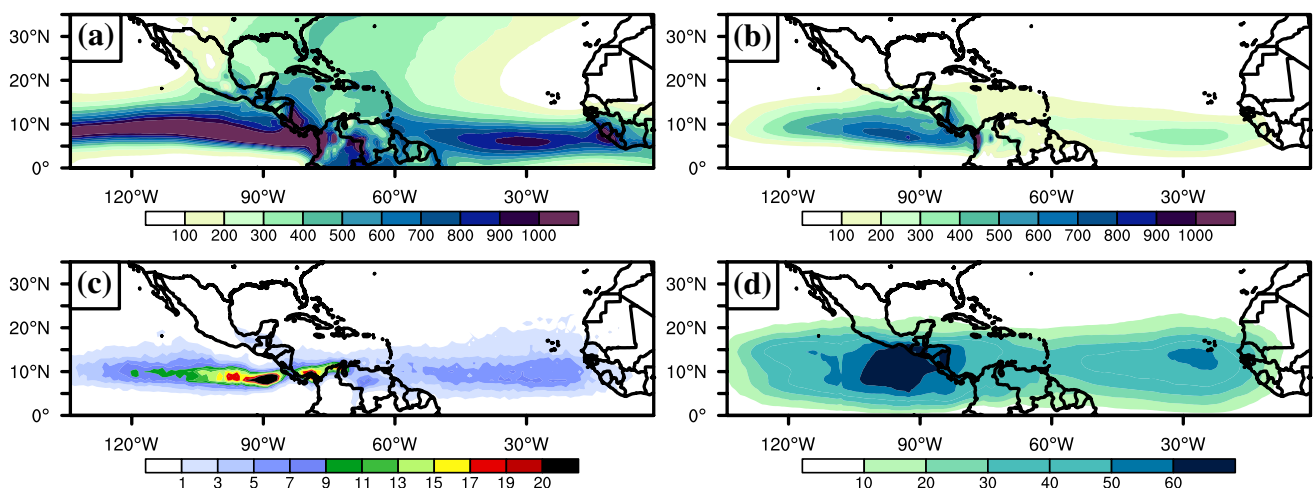
Fig. 2 **a** Summer rainfall (mm), **b** summer rainfall (mm) produced by easterly waves, **c** annual average easterly wave track density, and **d** contribution (%) of easterly waves to summer rainfall. Data are shown for the 1980–2013 period using ERAI data

EW density was computed as the number of tracks per unit area (1° × 1°) and per year (from May to November), as shown in Fig. 2c. Both coasts of Panama and NSA region experienced the highest density of EWs when compared to other continental regions such as southern Mexico or the coast of Africa. Apart from providing triggers for tropical cyclogenesis, EWs are significant contributors to regional seasonal precipitation. Their contribution is defined as the division of the seasonal EW rainfall by the total summer rainfall and then, multiplied by 100%. Figure 2d points out that EW contribution varies regionally. EWs can contribute more than 60% of summer rainfall over ENP and at least 50% over Costa Rica and Panama. Over southern Mexico and NSA their contribution can vary from 30 to 50% of the total seasonal rainfall (Fig. 2d). Thus, EWs should be essential elements of the hydrological cycle over TAs, since they act as highly convective systems and produce at least 20% of regional precipitation.

Surface stations and buoys that have information during the 1998–2013 period were analyzed. The analysis began in 1998 because the TAO/TRITON and PIRATA projects were launched operationally from 1998. The mean of EW contribution was computed as mentioned above. A surface station or buoy is affected by an EW when it is inside a box of 7.5° from the EW center defined by the TRACK technique and their contribution was averaged considering 16 years (from 1998 to 2013). This analysis supports the results using reanalysis data. EWs can produce more than 60% of seasonal rainfall over the ENP. However, as they move westward, their contribution decreases. Over the Central American region and MDR, EWs can contribute up to 60% of the rainfall (Fig. 3). TCs can also have an impact on the seasonal accumulated amount over MDR, but the most important contributors to summer rainfall are EWs. Over southern Mexico and NSA, their contribution to seasonal precipitation varies regionally. The main contribution over NSA is located in the north of the region. For example, EWs over the north of Colombia and Venezuela can contribute up to 50% (Fig. 3).

3.2 Relationships between ENSO, regional rainfall and TC activity over the northern South America

The yearly accumulated summer precipitation or seasonal rainfall over NSA varies from 500 mm to more than 1000 mm (blue bars in Fig. 4). This variability is also linked to the changes in summer rainfall produced by EWs (green bars in Fig. 4), since the correlation between accumulated summer precipitation and seasonal EW rainfall over NSA is r = 0.63 at a 99% level of confidence for the 1980–2013 period. The number of EW days, defined as the yearly sum of days when EW passages over a region, also shows that the variability is well-correlated with the seasonal EW precipitation over this region for the whole period (r = 0.52 at a 99% level of confidence). For example, during the years when the seasonal rainfall was below normal, such as 1983 and 2005, the summer precipitation produced by EWs was also low and EW days were less than 20 over NSA (Fig. 4). This is far below the average of 33 days. Thus, it is demonstrated that changes in EW frequency over NSA may lead to large interannual variations of precipitation.

The MDR is the region with the highest proportion of EWs becoming TCs. Instead of reaching the NSA region, some of these TCs can curve and carry moisture from the TAs to the subtropical mid-Atlantic Ocean or the eastern US, depending on the TC track. In that sense, TC circulations can also reduce the chances of rain over NAS by inducing moisture divergence over this region, particularly when the TC tracks are over the mid-Atlantic Ocean. Our hypothesis is that more TC days over MDR mean fewer EWs reaching NSA and consequently, less EW days affecting this region. However, this relationship is only valid for some years, such as 1987, 2005 and 2012. The opposite occurs for some years, such as 1985, 2006 and 2013. The correlation between TC days over MDR and EW days over NSA is 0.23 for the whole period and it is not statistically significant. It is possible that this correlation is low because the EW–TC relationship is strongly modulated by interannual climate oscillations, as the ENSO.

ENSO is an important climate forcing that drives changes in atmospheric circulations over the TAs, inducing positive or negative anomalies of accumulated rainfall,

Fig. 3 Climatological annual contribution (%) of EWs to summer rainfall during the 1998–2013 period using surface station data
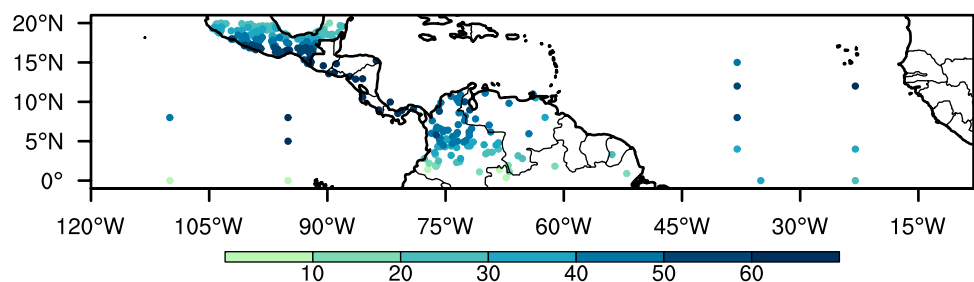
Fig. 4 Accumulated summer precipitation (mm, blue bars) and accumulated summer precipitation produced by easterly waves (mm, green bars) over northern South America, using ERAI. The blue line represents the accumulated days of TCs over the main development region and the red line represents the yearly easterly wave days over the Northern South America during the 1980–2013 period
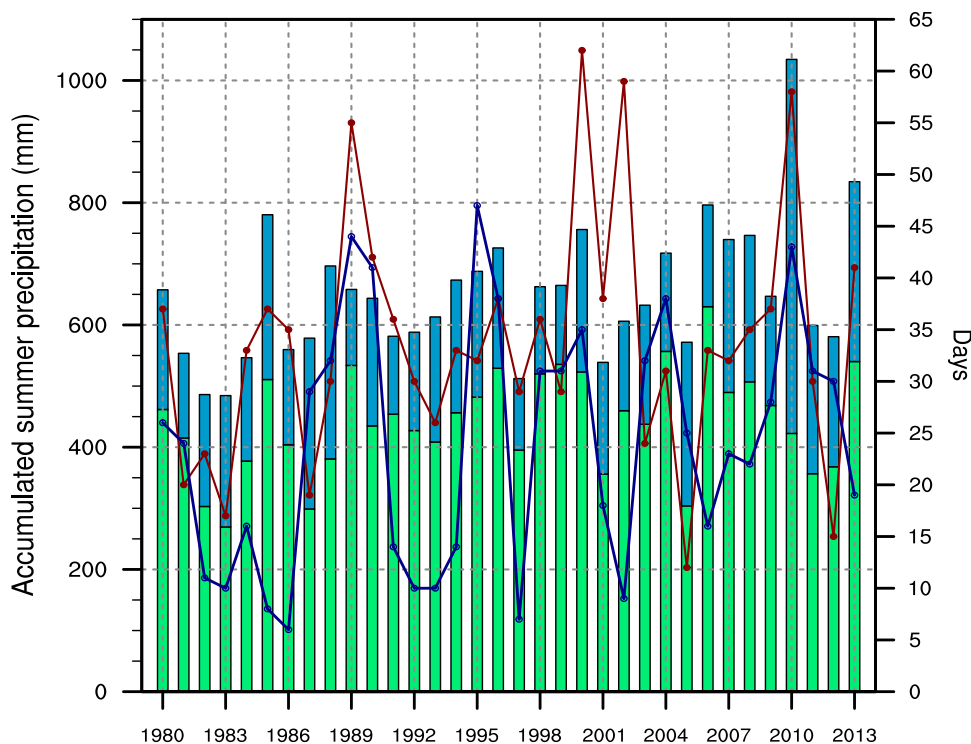

Table 1 Years when the ENSO phase was El Niño, neutral conditions, and La Niña between 1980 and 2013

El Niño	Neutral				La Niña
1983	1980	1992	2001	2008	1988
1987	1981	1993	2003	2011	1995
1991	1984	1994	2005	2012	1998
1997	1985	1996	2006	2013	1999
2002	1990	2000	2007		2010

depending on the phase. During the 1980–2013 period, 5 years were defined as El Niño and five as La Niña.

However, some weak El Niño and La Niña events were not considered in our study. Neutral conditions cover 19 years (Table 1). Firstly, the ENSO impact on the seasonal precipitation over NSA is determined.

Seasonal precipitation anomalies over NSA are defined as the subtraction of the accumulated rain value in a given year minus the average of the summer rainfall over this region for the 1980–2013 period. The behavior of the regional precipitation under the three phases of ENSO was determined by averaging the anomalies in rainfall over NSA during the years that each phase was active. The yearly number of TC days corresponds to the sum of the days when TCs are over the MDR. The anomalies are created by averaging the yearly number of TCs days and then subtracting the average from the TC days in a given year.
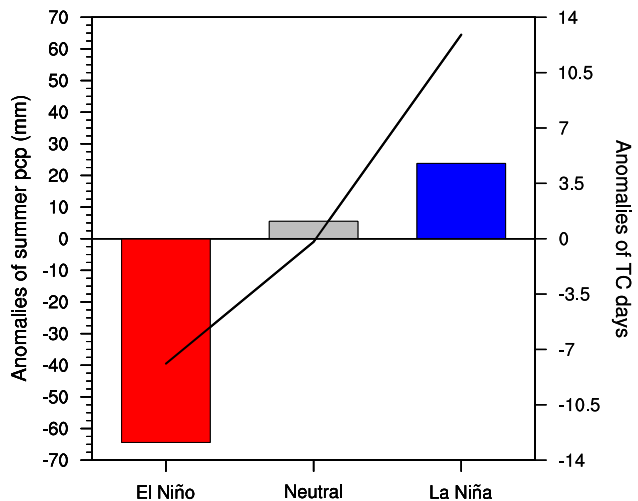
Fig. 5 Summer rainfall anomalies (mm) in northern South America under the ENSO conditions during the 1980–2013 period, using ERAI. The black line represents the anomalies in the number of TC days over the main development region under the ENSO conditions

In general, Fig. 5 shows that El Niño brings dry conditions and La Niña brings wet conditions to the NSA region.

Under El Niño years, the chances for deep convection decrease due to the enhancement in wind shear (Camargo et al. 2007) and the number of TC days over the MDR also diminishes. Under La Niña years, the atmospheric conditions are more favorable to deep convection when compared to neutral conditions and the number of TC days over the

MDR increases. By modifying the large-scale circulation over TAs, ENSO strongly influences the regional climate variability over NSA. Under neutral conditions, a slightly opposed signal exists between the anomalies of seasonal precipitation over this region and anomalies in TC days over the MDR during the whole period (Fig. 5). In fact, considering only neutral ENSO conditions during the whole period, the correlation between anomalies in seasonal precipitation over NSA and anomalies in TC days over the MDR is -0.5 at 95% level of confidence.

EW track density and their associated rainfall under ENSO phases were examined. The anomalies of easterly wave track density were computed as the difference between the average of track density for each ENSO phase and the climatological track density for the 1980–2013 period. Under El Niño conditions, fewer EWs reach NSA (Fig. 6b). This result is consistent with Bengtsson et al. (2006), who used ERA40 reanalysis to show negative track density anomalies under the warm phase of ENSO over the coast of NSA. However, the opposite occurs under La Niña conditions (Fig 6f), more EWs reach NSA. A strong dipole in the anomalies of easterly wave track density appears over the MDR under El Niño and La Niña conditions but inverted for each ENSO phase. This could suggest that the ENSO could modulate waveguide activity and determine which one is more active, depending on the ENSO phase. The physical mechanism that drives this dipole and the EW activity over MDR remains as future work. Under Neutral conditions, no pattern in the anomalies of easterly wave track density is noticeable.

Some El Niño years show fewer EW days than average, corresponding to a negative change (defined as negative anomalies from average) in EW contribution to seasonal rainfall over NSA. While some El Niño years show more EW days, meaning a positive contribution (Fig 7a). During 1997, although fewer EW days affected NSA, most of the seasonal precipitation was produced by EWs. Figure 4 also shows this, meaning that EWs were the main moisture carriers in 1997. Overall, the anomalies in TC days over MDR tend to be negative under El Niño, except for 1987 (Fig. 7a). The EW–TC rainfall relationship holds in 1987, 1991 and 2002, which shows that even during El Niño events, the number of TCs over MDR and EW days over NSA are highly related. This relationship can dominate wet or dry seasons over the NSA region, depending on the number of EWs that reach the region, since the EW days and accumulated seasonal rainfall over this region are greatly correlated.

Under La Niña conditions, TC days over MDR and EW days over NSA are higher than normal (Fig 7b). Despite the high TC activity over MDR, the EW contribution tends to be higher than normal (Fig 7b), suggesting that large-scale atmospheric conditions are strongly favorable for intense convection over NSA during 1995, 1998 and 1999, and the TC-drying effect is overwhelmed for those years. However, this relationship does not hold for the stronger La Niña events of 1988 and 2010. During 1988, the anomalies in EW days are negative over NSA and so is their contribution to seasonal precipitation (Fig 7b). Based on Arias et al. (2015), the intensification of the Chocó Jet and the reduction in the
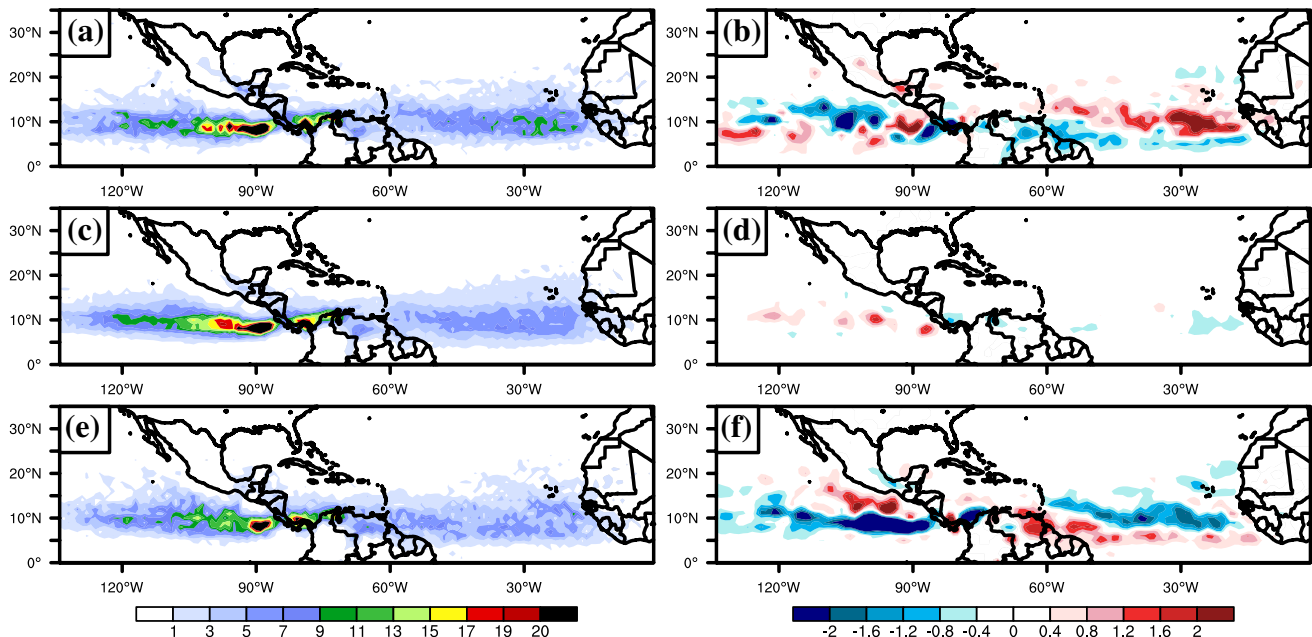
Fig. 6 Annual average easterly wave track density for: **a** El Niño years, **c** neutral years, **e** La Niña years during the 1980–2013 period and the anomalies of easterly wave track density for **b** El Niño years, **d** neutral years and **f** La Niña years

magnitude of the CLLJ led to an anomalous wet season over NSA in 2010, mainly over Colombia. The latter indicates that La Niña conditions are not the only responsible driver for this atypical wet year. This is also supported by Fig. 4, which shows that the rainfall produced by EWs was moderate when compared to non-EW precipitation in 2010. Therefore, our results are consistent with Arias et al. (2015).

The EW contribution to accumulated summer rainfall exhibits considerable interannual variability under neutral conditions (Fig. 7c). The anomalous EW day frequency over NSA and anomalous TC days over MDR had similar sign in most of the years from 1980 to 2000 (Fig. 7c). However, after the year of 2000, the EW–TC rainfall relationship strengthens, which suggests that a decadal oscillation could
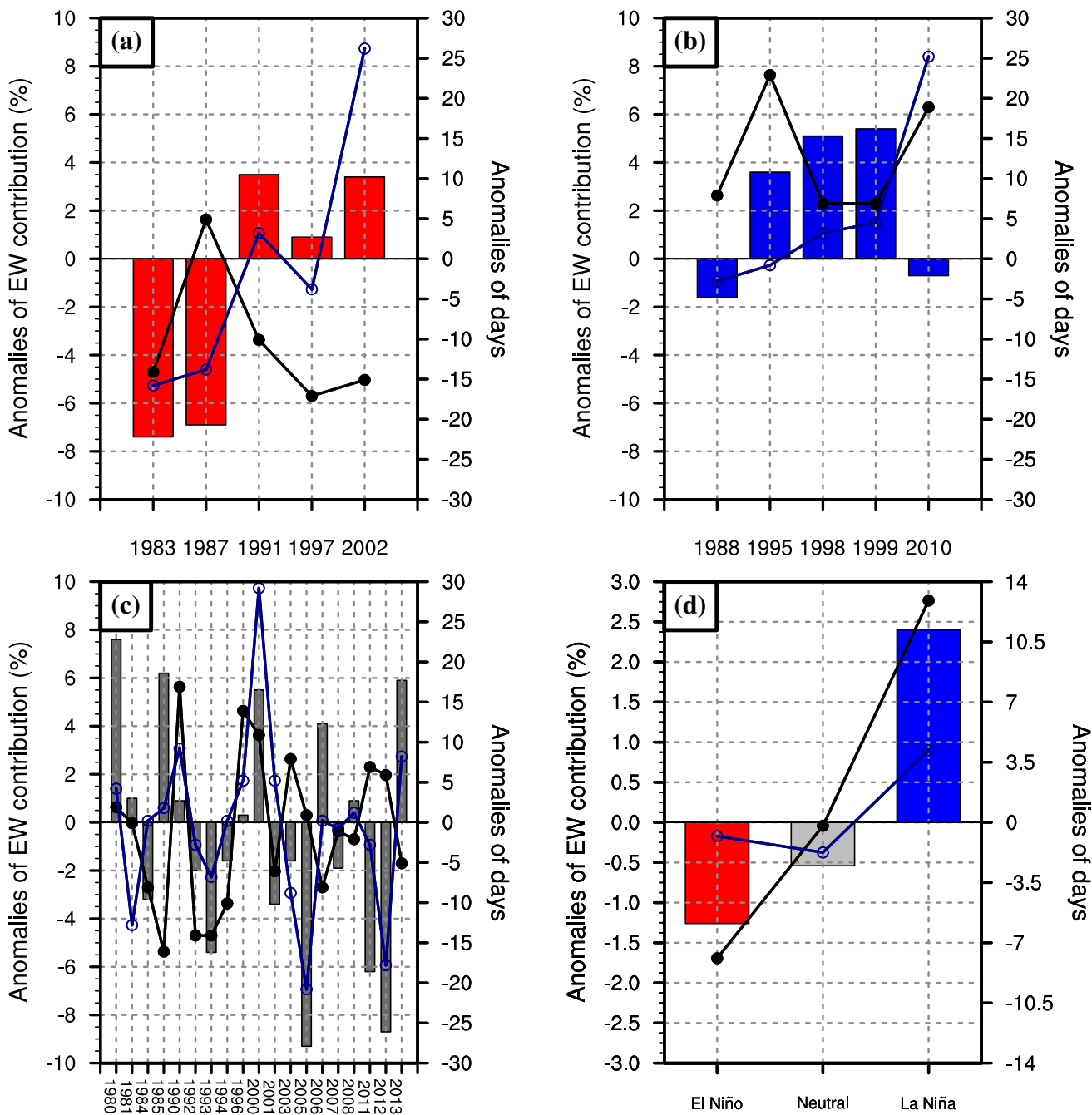
Fig. 7 Anomalies of easterly wave (EW) contribution (%) to seasonal rainfall over northern South America for: **a** El Niño years, **b** La Niña years and **c** Neutral years and **d** the three ENSO phases during the 1980–2013 period. The blue line represents the anomalies in EW days over northern South America and the black line represents the anomalies in TC days over the main development region

play an important role in modulating this relationship under neutral ENSO conditions.

In summary, El Niño years result in less precipitation produced by EWs over NSA and a reduction in their activity (Figs. 6b, 7d), while La Niña years result in more precipitation produced by EWs over NSA and an increase in their activity (Figs. 6f, 7d). Under neutral conditions, our proposed EW–TC rainfall relationship only becomes apparent after the year 2000.

3.3 Decadal modulation of the relationship between tropical cyclones and regional precipitation

The correlation between seasonal rainfall over NSA and TC days over MDR changes across the decades. The correlation for the decade 1980–1989 is 0.61, for 1990–1999 is 0.60, significant at a 95% level of confidence and for the 2000–2013 period is -0.1 (non-significant). However, after 2000, TCs and seasonal rainfall are anti-correlated. The long-timescale variation in the correlation suggests that a long-term mode of climate variability may play an important

role in the modulation of EW and TC frequency. The latter is partly supported by the analysis of the relationship between the EW contribution to accumulated summer rainfall over NSA and the anomalies of TC days over MDR under neutral conditions, which suddenly changes after the year of 2000 (Fig. 7c). Here, the AMO is explored as the main decadal modulator over the Atlantic Ocean, whose index turned positive from the year 1995.

To assess the potential influence of the AMO on the atmospheric circulation for the 1980–2013 period, the negative phase of AMO is defined as the years whose averaged summer index is lower than -0.103 °C (threshold that characterizes the values that are in the lower tercile of the AMO distribution) and the positive phase exists when the yearly averaged value is greater than 0.104 °C (threshold that characterizes the values that are in the upper tercile of the distribution). The AMO modifies SSTs over a large portion of the Atlantic Ocean. However, the SST variance depends on the location and time of the year. So, the anomalies are standardized considering the whole period. Nine years before 1995 are considered as AMO− and 10 years are defined as AMO+ (Table 2).

The main dynamical factor that dominates the convection over the tropical Atlantic is the vertical wind shear (Camargo et al. 2007). Thus, the anomalies of vertical wind shear are examined to explore shear as a possible mechanism through which AMO has influence.

Figure 8a reveals that under AMO+ conditions, the standardized SST positive anomalies are present across the entire tropical Atlantic Ocean and the anomalies of vertical wind shear are negative, principally over the NSA region and its Atlantic coast, where the largest values are around -1.2 m/s. This promotes tropical convection and consequently,

Table 2 Years when AMO index was in the lower tercile, defined as AMO −, and years when AMO index was in the upper tercile, defined as AMO +

AMO −		AMO +	
1982	1991	1995	2006
1983	1992	1999	2007
1984	1993	2001	2008
1985	1994	2003	2009
1986		2005	2013

Fig. 8 Standardized anomalies of sea surface temperature (°C, shaded) and anomalies of vertical wind shear (m/s, green contours) for **a** years when their AMO index was in the upper tercile and **b** years when their AMO index was in the lower tercile. Dashed green lines represent negative anomalies of wind shear, the bold line represents the value of zero and the continuous green lines represent positive anomalies
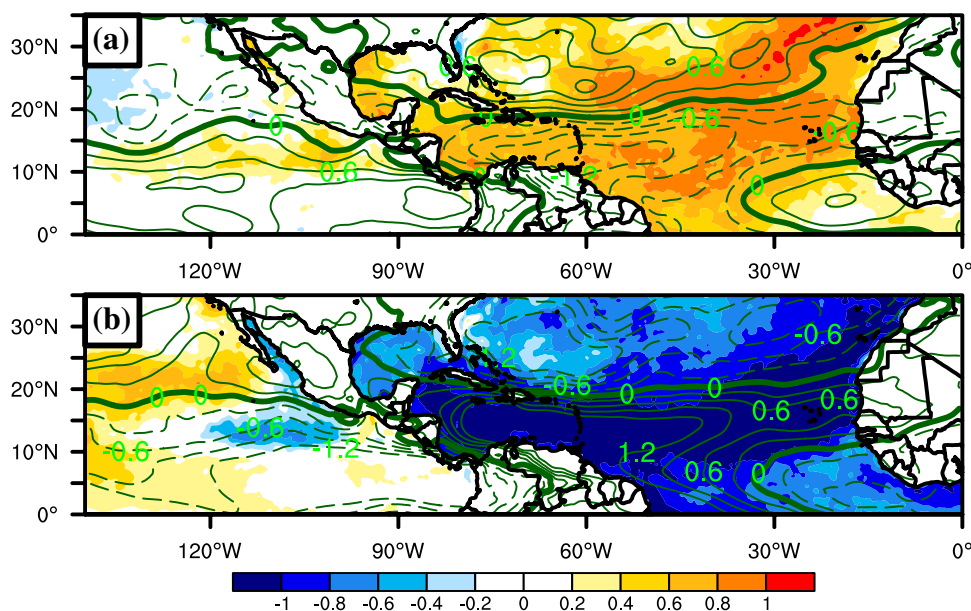
produces more rainfall. On the other hand, the standardized SST anomalies are negative over the Atlantic Ocean and strong positive anomalies of vertical wind shear exist over the Atlantic coast of NSA and its adjacent landmass under AMO− conditions (Fig. 8b). These conditions are unfavorable for deep convection. Our results are consistent with Goldenberg et al. (2001) who identified vertical wind shear and SSTs as dominating TC frequency over the North Atlantic Ocean. Goldenberg et al. (2001) also suggests that more intense hurricanes can occur during AMO+, which indicate the existence of intense and well-defined TC circulations and therefore, the TC-drying effect may be stronger under AMO+ conditions than under the AMO− phase.

3.4 Relationships between easterly waves, tropical cyclones, and regional rainfall during recent neutral ENSO years

According to the results for the AMO phases, the EW–TC rainfall relationship does not hold in neutral years before 1995 because of the inhibited convection induced by AMO− conditions. Under such conditions the TC circulations over MDR and curving into the mid-Atlantic may not be strong enough to have a well-defined drying effect. However, the EW–TC rainfall relationship holds for neutral years from 2001 onwards.

Neutral years of high TC activity over MDR (2005, 2011 and 2012) and neutral years of low TC activity over MDR (2006, 2008 and 2013) are analyzed to explore the atmospheric dynamics that drive the changes in EW contribution and therefore, changes in regional precipitation, without considering a climate forcing as ENSO. Figure 9b shows that during years of high TC activity, the anomalies in the precipitation associated with EW tracks are below normal (Fig. 9a). The Caribbean region and NSA experience negative anomalies of vertically integrated moisture flux, but the

eastern US is affected by a large anomalous moisture flux (Fig. 9c). The latter results in less seasonal EW rainfall over TAs when compared to relatively inactive TC seasons over MDR in neutral years (Fig. 9d).

During years of relatively low TC activity over MDR, EWs produce up to 125 mm above the average over the Caribbean region and NSA (Fig. 9d, e). This results from positive anomalies of integrated moisture flux over these regions (Fig. 9f). Interestingly, the accumulated summer precipitation produced by EWs over the ENP also increases during the years of relatively low TC activity over the MDR and diminishes during active TC seasons (Fig. 9a, d).

These results suggest that under AMO+ and ENSO neutral conditions, TC activity over MDR could serve as an indicator of dry summer seasons over NSA, when the strong interannual climate signal of ENSO is absent.

4 Results: easterly wave contributions to seasonal rainfall in a RCM ensemble

This section complements the observational analysis in the previous section and presents an analysis of a multi-physics RCM ensemble simulation. Each ensemble member produces a slightly different atmospheric response to the same SSTs. This presents an opportunity to (1) develop understanding of the extent to which RCMs can capture the EW–TC rainfall relationships, and (2) assess the strength of the physical mechanisms to different representations of physical processes.

4.1 Frequency of easterly waves

All members simulate adequately the EW activity over the MDR (Fig. 10) when compared to ERAI (Fig. 10l). However, all the members underestimate the simulated EW track density over the ENP. The members ck6 m, cn6y and rn6y
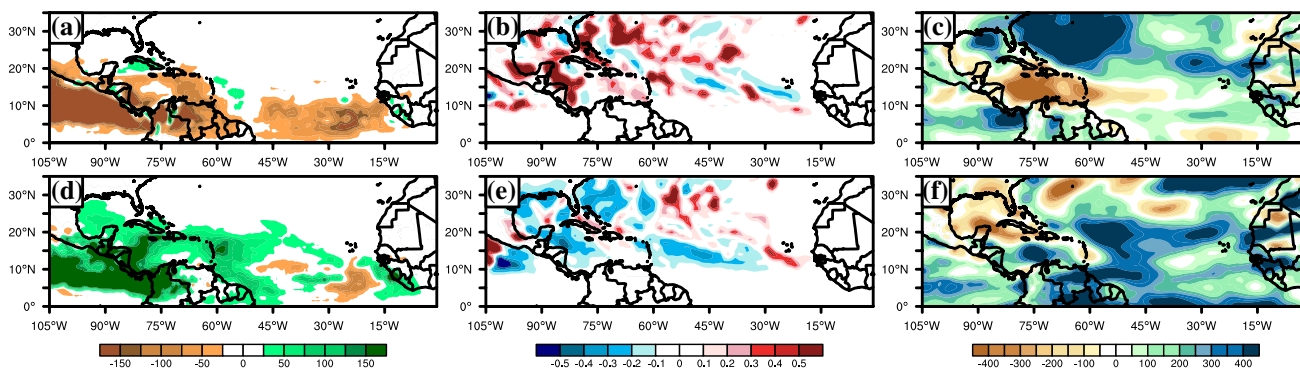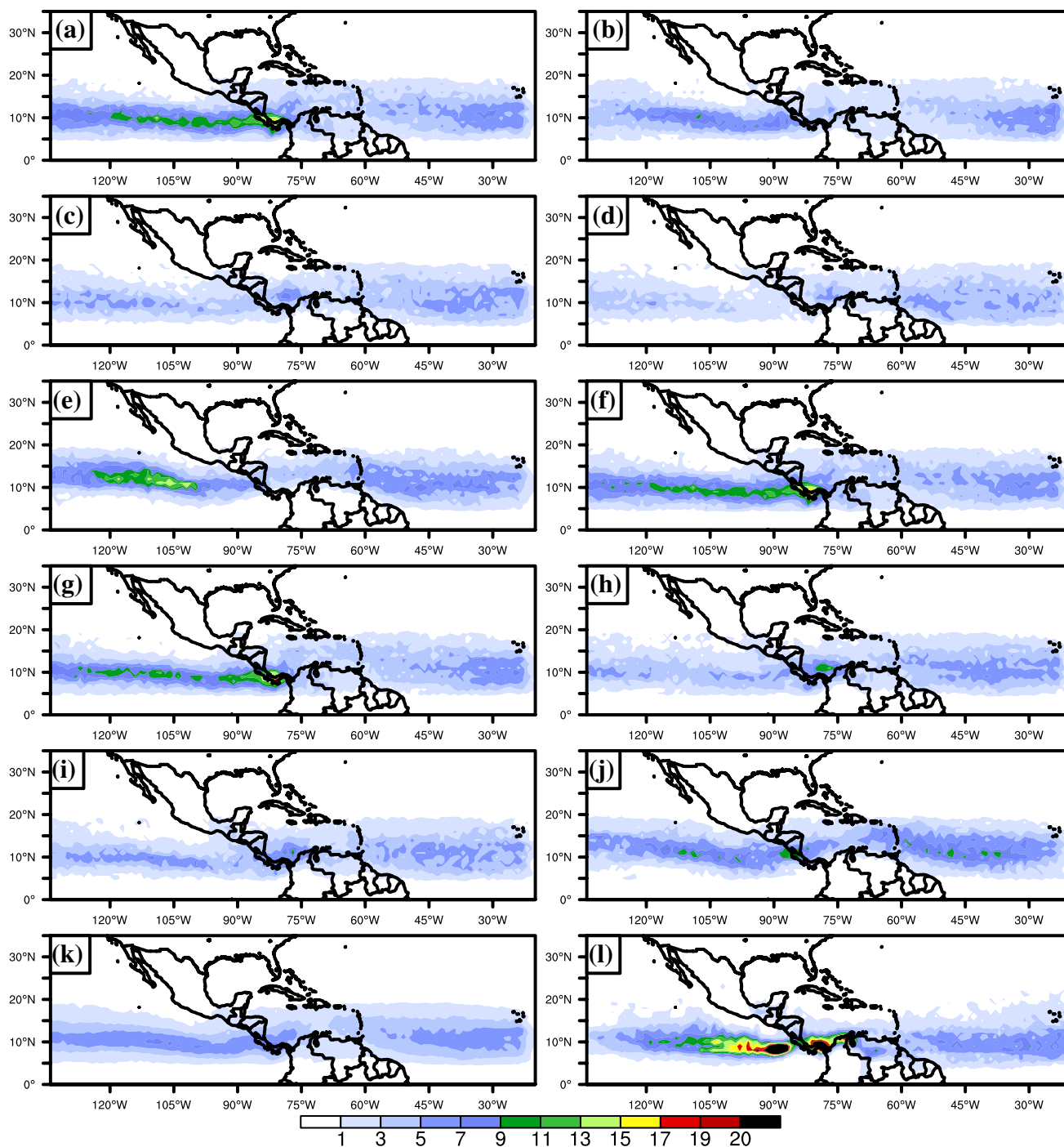

Fig. 9 Anomalies of seasonal rainfall (mm) associated with easterly wave tracks (**a**, **d**), anomalies of TC density (**d**, **e**), and anomalies of vertically integrated moisture flux (**c**, **f**, kg/m^2 s) for years of high TC activity: 2005, 2011 and 2012 (upper row), and years of low TC activity: 2006, 2008 and 2013 (bottom row) over the main development region

Fig. 10 Annual average density of easterly wave tracks in ten members of the RCM ensemble: **a** ck6m, **c** cktm, **e** cn6y, **g** cnty, **i** ctty, **b** rk6m, **d** rktm, **f** rn6y, **h** rnty, **j** rtty, **k** ensemble mean and **l** ERAI during the 1990–2000 period

simulate their maximum EW density westwards of the ERAI maximum (Fig. 9a, e, f), but they capture EW activity better in contrast to the other members. This indicates that WRF Single-Moment 6-Class microphysics scheme has a great impact on the EW activity.

The hurricane matching technique revealed that 50% of TCs develop from EWs over the North Atlantic Ocean and 71% over the Eastern Pacific Ocean by using the ERAI reanalysis and HURDAT database (Fig. 11). Our results over the Atlantic basin are consistent with Agudelo et al. (2011) and Schreck et al. (2012), since these studies estimate that
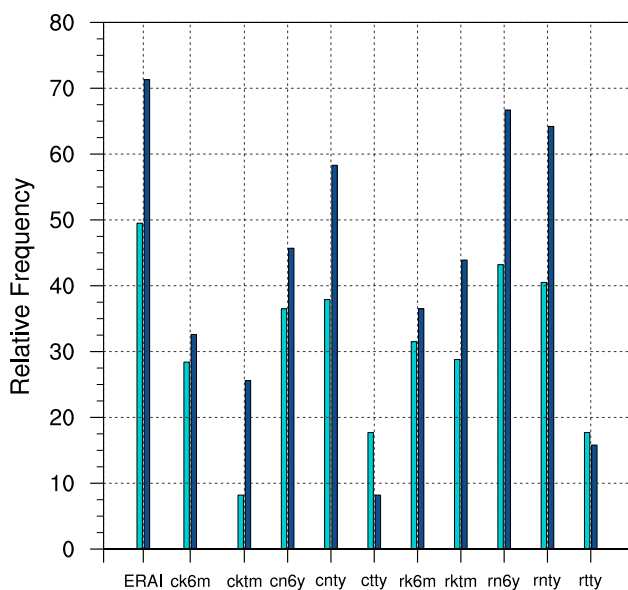
Fig. 11 Percentage (%) of easterly waves that become TCs over the North Atlantic basin (light blue) and Eastern North Pacific Ocean (dark blue) according to the ERAI reanalysis and ten members: ck6m, cktm, cn6y, cnty, ctty, rk6m, rktm, rn6y, rnty and rtty during the 1990–2000 period

50–60% of the tropical cyclogenesis is produced by the TD-type waves over the Atlantic basin. Nevertheless, Schreck et al. (2012) found a smaller percentage of TCs that originate from EWs over the Pacific basin (40–65%). Based on our results using ERAI, we suggest that EWs are the dominant tropical modes that produce TCs over the ENP, which also yield up to 70% of the accumulated summer rainfall over this region.

For the RCM outputs, all ensemble members underestimate the tropical cyclogenesis produced by EWs when compared to ERAI. The only two members that reasonably simulate TCs coming from TD type waves (more than 40%) are rn6y and rnty. The RRTMG/New Simplified Arakawa-Schubert/Yonsei University combination has an impact on the generation of tropical cyclogenesis (Fig. 11). Intriguingly, these two members produced fewer TC tracks when compared to the rest of the members (Bruyère et al. 2017). On the other hand, the worst-performing members for simulating EWs as precursors (cktm and ctty) adequately capture TC tracks (Bruyère et al. 2017). Further research is needed to determine this misrepresentation.

4.2 Simulated easterly wave contributions to rainfall

The simulated EW rainfall varies substantially among the ensemble members. While four members, cn6y, rn6y, cnty and rtty, captured adequately the EW precipitation over the

ENP (Fig. 12e–g, j), all members produced too low precipitation (less than 200 mm) over the Atlantic Ocean and its continental landmass, as NSA. Only two members—cn6y and rtty—reasonably capture EW precipitation over the MDR (Fig. 12e, j). It seems that the EW track density is not related to the skill of representing EW rainfall, since all the members simulate the EW activity over this region appropriately, but only two members represent the EW precipitation adequately. This suggests that the RCM produces the wind patterns associated with EW horizontal structure, but that these tropical waves are too dry.

Despite a misrepresentation of EW rainfall over the MDR, all members overestimate the EW contribution (more than 60%) to seasonal rainfall (Fig 13). In general, the percentage of EW contribution over NSA is well-represented by the ensemble (Fig. 13k) but poorly represented over the ENP. The members cn6y and rtty, which are the only members that adequately simulate the EW rainfall over the MDR, do not have a good skill to simulate the EW contribution to seasonal precipitation over the NSA appropriately (Fig. 13e, j). In addition, the EW contribution over the Central American region is underestimated by members rk6 m, cktm, rktm, cn6y, rnty, ctty and rtty.

4.3 Simulated relationships between ENSO, regional precipitation and tropical cyclone activity

Some RCM ensemble members show that they can simulate the EW track density over the ENP adequately (Fig. 10), but they cannot capture the EW contribution to accumulated summer precipitation over this region. This suggests that most of the EWs are simulated as dry waves. On the contrary, some members have problems simulating EW track density over NSA, but they reproduce a reasonable EW contribution over this region.

The interannual variability of the EW–TC rainfall contribution is explored here for each ENSO phase. During the 1990–2000 period of the RCM simulations, only 1991 and 1997 were El Niño years, and 1995 and 1999 were La Niña years (Table 1). For the same period, the years 1990, 1992, 1993, 1994, 1996 and 2000 are ENSO neutral years (Table 1).

During El Niño years, the RCM ensemble shows a negative change in the EW contribution to seasonal precipitation over NSA (Fig. 14a), which demonstrates that EWs simulated by RCM members produce less rainfall than normal under these conditions. The performance of the anomalies in EW days over NSA has a good skill when compared to observations (Fig. 7), since their anomalies are like those observed, but for the 1980–2013 period. In addition, the RCM ensemble also indicates that, under El Niño conditions, MDR TC days are fewer, which also
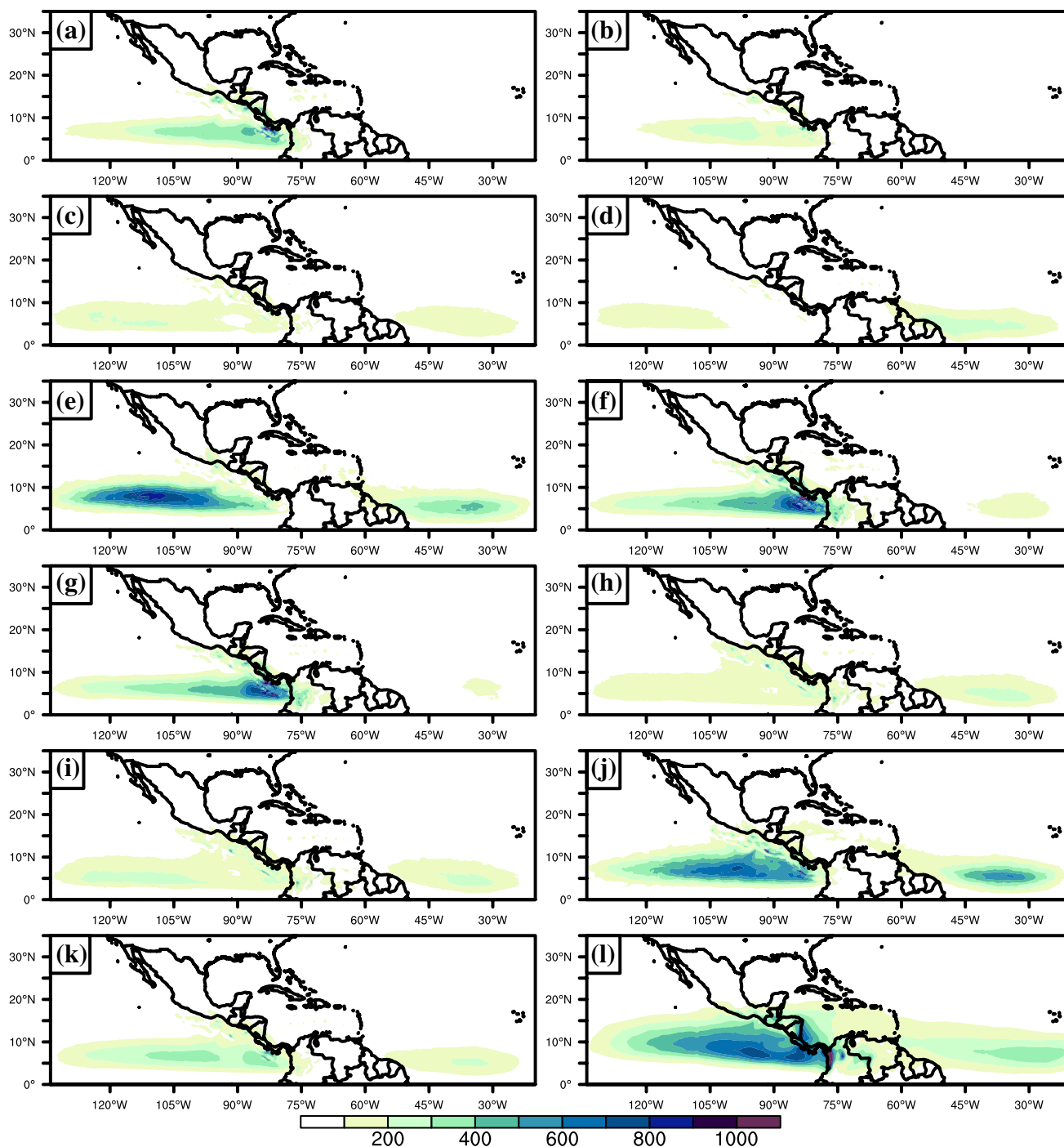
Fig. 12 Rainfall (mm) produced by easterly waves in ten members of the WRF ensemble: **a** ck6m, **c** cktm, **e** cn6y, **g** cnty, **i** ctty, **b** rk6m, **d** rktm, **f** rn6y, **h** rnty, **j** rtty, **k** ensemble mean and **l** ERAI during the 1990–2000 period

agrees with observations (Fig. 7a). For La Niña conditions EWs generally produce precipitation above normal over NSA and TC days are also generally active over MDR (Fig. 14b), as we concluded in Sect. 3.2. However, slightly negative anomalies of EW days in 1998 are simulated

under these conditions. Therefore, EWs over NSA and TCs over MDR are reasonably well represented by the RCM ensemble in the two ENSO phases.

During neutral years, the EW–TC rainfall relationship is dominant in 1993, 1994 and 2000 (Fig. 14c), which
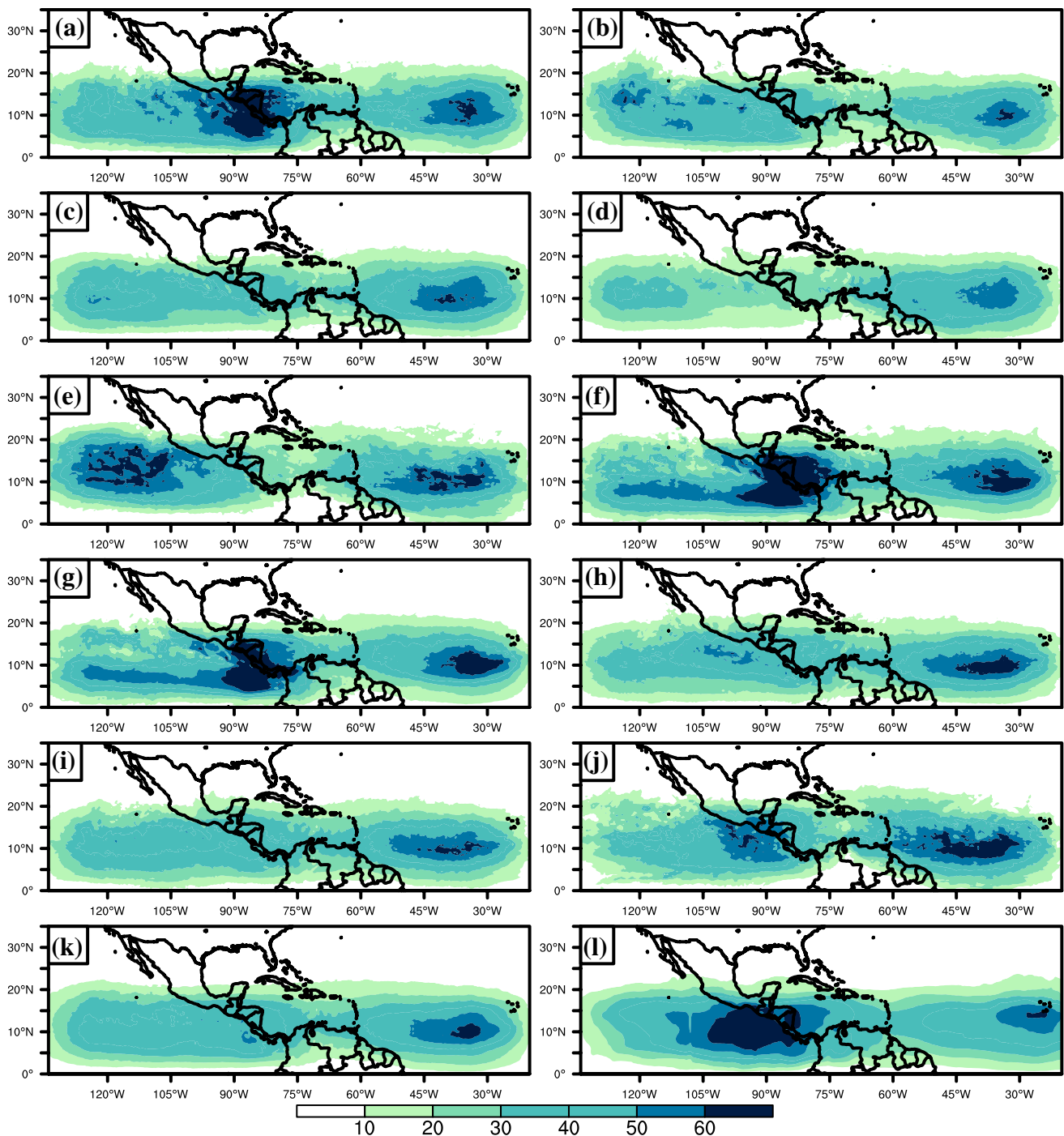
Fig. 13 As Fig. 12 but for the contribution (%) of easterly waves to summer rainfall

is different from the observed relationship in those years (Fig. 7c). Moreover, the variability in EW contribution and EW days during neutral ENSO phase is less than in observations (Fig. 7c).

In summary, the RCM ensemble reproduces adequately the atmospheric response to La Niña and El Niño SST conditions. Figure 14 reveals that the RCM can capture most of

the EW and TC characteristics over NSA and MDR under different ENSO phases. Our previous results are consistent with this figure because convection is inhibited under El Niño conditions and so is the EW contribution to summer season over NSA (Fig. 14d). Furthermore, EW convection over NSA is enhanced under La Niña conditions.
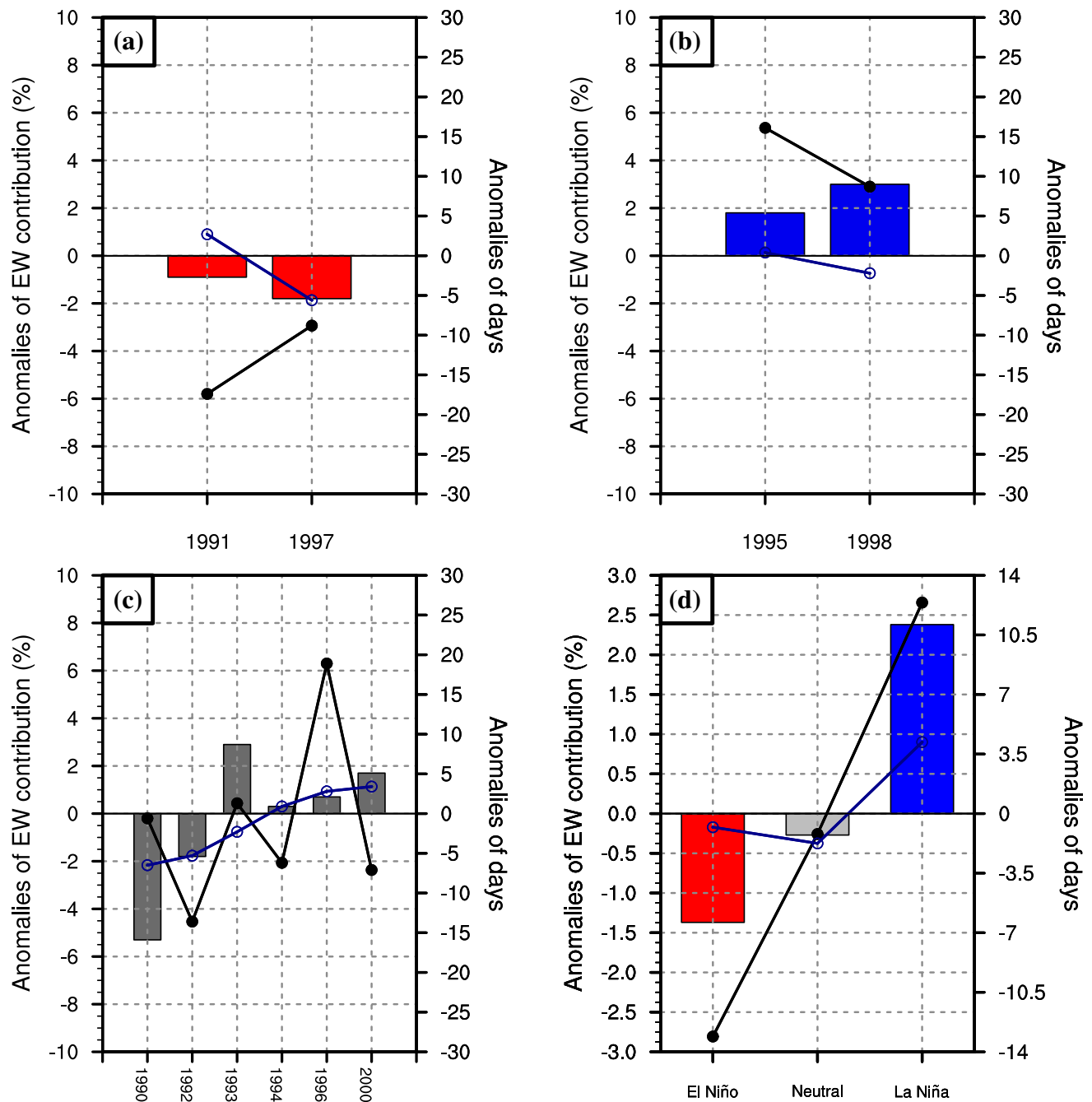
Fig. 14 Anomalies of EW contribution to seasonal rainfall (%) for the WRF ensemble under **a** El Niño conditions, **b** La Niña conditions, **c** neutral conditions, and **d** the three phases of ENSO during the 1990– 2000 period. The blue line represents the anomalies in EW days over NSA and the black line represents the anomalies in TC days over the MDR

The relationship between TC days over MDR and NSA seasonal rainfall holds across the ensemble. The correlation between TC days over MDR and seasonal rainfall over NSA is 0.61 in ERA-I and 0.60 during neutral years for the 1990–2000 period. The members cn6y, cnty, rk6 m and rktm, rn6y, rnty and rtty (70% of the members) capture this signal (Table 3).

In summary, the RCM adequately captures the regional climate variability over the TAs. In particular, the EW–TC rainfall relationships seen in observations are robust to the different physical representations in the multi-physics ensemble, as is the relationship between MDR TC days and accumulated seasonal rainfall over NSA. RCMs may

Table 3 Correlations between TC days over MDR and seasonal rainfall over NSA at 95% level of confidence

	1990–2000	Neutral years
ERAI	0.61	0.60
ck6m	−0.02	0.19
cktm	0.16	−0.15
cn6y	0.88	0.90
cnty	0.46	0.57
ctty	0.01	−0.16
rk6m	0.49	0.32
rktm	0.40	0.71
rn6y	0.50	0.42
rnty	0.47	0.62
rtty	0.72	0.80

therefore provide useful information about the regional climate variability of the TAs.

5 Summary and conclusions

Tropical cyclones (TCs) and Easterly Waves (EWs) are key phenomena over the tropical Americas (TAs) for their importance in transporting moisture. EWs are important transporters of humidity to northern South America (NSA), the Caribbean Sea, Central America, and southern Mexico, collectively defined as TAs landmass. In particular, the accumulated seasonal rainfall depends on EW activity, since they produce up to 50% of the accumulated summer precipitation over NSA.

An observational analysis showed that El Niño-South Oscillation (ENSO) dominates interannual variability over TAs. Under strong El Niño conditions, induced subsidence inhibits deep convection over TAs. Under strong La Niña conditions, the lack of subsidence promotes deep convection and enhanced rainfall over NSA (Arias et al. 2015). Under ENSO neutral conditions the EW contribution to interannual variability can become important. We find a relationship between TC days over MDR and the EW contribution to accumulated seasonal rainfall under neutral ENSO conditions, but only after the year 2000. In this period, more TC tracks that curve into the mid-North Atlantic transport more moisture into the subtropics or mid-latitudes. This reduces the chance of rain over the continental TAs because the number of EW days reaching this region is reduced. This is defined in this paper as the EW–TC rainfall relationship. The opposite effect occurs under low TC activity over MDR. However, this relationship is overwhelmed under strong El Niño or La Niña events and it is only valid under AMO+ conditions. AMO+ enhances tropical convection because the SSTs are anomalously warm and the vertical wind shear is

anomalously low. The EW–TC rainfall relationship vanishes under AMO− conditions because cool SSTs and strong vertical wind shear is more intense, preventing deep tropical convection from organizing.

Additional comparative studies are needed to fully understand how robust the results are to details of our analysis. In particular, sensitivity should be tested to the definition of EW rainfall based only on rainfall associated with the positive phase of the waves, to understand the extent to which this definition underestimates EW contributions to rainfall.

To complement the observational analysis, a multiphysics RCM ensemble simulation was used to (1) develop understanding of the extent to which RCMs can capture the EW–TC rainfall relationships, and (2) assess the strength of the physical mechanisms to different representations of physical processes. Our analysis of observations showed that 50% and 70% of TCs come from EWs over the North Atlantic and North Eastern Pacific Ocean, respectively. Most of the ensemble members were able to reasonably capture EWs as precursors of cyclogenesis in both basins. Whereas the simulated EW precipitation over land is poorly represented, the EW contribution to seasonal rainfall over TAs landmass is adequately captured by most of the members. The atmospheric responses to ENSO are also well simulated by the members as demonstrated by the analysis of TC days over MDR, EW days over NSA and their contribution to seasonal rainfall. The positive correlation between TC days over MDR and seasonal precipitation over NSA during the period 1990–2000 was also adequately captured by 70% of the members. This indicates that the relationship is fairly robust to the different representations of physical processes.

Additional RCM simulations are needed to assess whether the EW–TC relationship is robust in other decades with other combinations of AMO and ENSO characteristics. Moreover, future work should further investigate the physical mechanisms that drive EW activity over TAs under AMO+/− conditions.

The findings of this research have implications for climate predictability. There is potential to predict rainfall over continental TAs based on predictions of TC activity over MDR (e.g., Klotzbach et al. 2011; Klotzbach et al. 2017) under neutral ENSO and AMO+ conditions.

References

Agudelo PA, Hoyos CD, Curry JA, Webster PJ (2011) Probabilistic discrimination between large-scale environments of intensifying and decaying African Easterly Waves. Clim Dyn 36:1379–1401

Arias PA, Martínez JA, Vieira SC (2015) Moisture sources to the 2010-2012 anomalous wet season in northern South America. Clim Dyn 45:2861–2884. https://doi.org/10.1007/s00382-015-2511-7

Barnston AG, Li S, Mason SJ, DeWitt DG, Goddard L, Gong X (2010) Verification of the first 11 years of IRI's seasonal climate forecasts. J Appl Meteorol Climatol 49:493–520

Bengtsson L, Hodges KI, Roeckner E (2006) Storm tracks and climate change. J Clim 19:3518–3543

Berry G, Thorncroft CD (2012) African easterly wave dynamics in a mesoscale numerical model: the upscale role of convection. J Atmos Sci 69:1267–1283

Berry G, Thorncroft C, Hewson T (2007) African easterly waves during 2004—analysis using objective techniques. Mon Weather Rev 135:1251–1267

Bruyère CL et al (2017) Impact of climate change on Gulf of Mexico Hurricanes. NCAR Technical Note NCAR/TN-535 + STR. https://doi.org/10.5065/d6rn36j3

Camargo SJ, Emanuel KA, Sobel AH (2007) Use of a genesis potential index to diagnose ENSO effects on tropical cyclone genesis. J Clim 20:4819–4834. https://doi.org/10.1175/jcli4282.1

Caron LP, Boudreault M, Bruyère CL (2015) Changes in large-scale controls of Atlantic tropical cyclone activity with the phases of the Atlantic multidecadal oscillation. Clim Dyn 44:1801–1821. https://doi.org/10.1007/s00382-014-2186-5

Cerveny RS, Newman LE (2000) Climatological relationship between tropical cyclones and rainfall. Mon Weather Rev 128:3329–3336. https://doi.org/10.1175/1520-0493(2000)128%3c3329:crbtca%3e2.0.co;2

Chen F, Dudhia J (2001) Coupling an advanced land-surface/hydrology model with the Penn State/NCAR MM5 modeling system. Part I: model implementation and sensitivity. Mon Weather Rev 129:569–585

Collins WD et al (2006) The Community Climate System Model Version 3 (CCSM3). J Clim 19:2122–2143

Crétat J, Vizy EK, Cook KH (2015) The relationship between African easterly waves and daily rainfall over West Africa: observations and regional climate simulations. Clim Dyn 44:385. https://doi.org/10.1007/s00382-014-2120-x

Crosbie E, Serra Y (2014) Intraseasonal modulation of synoptic-scale disturbances and tropical cyclone genesis in the eastern North Pacific. J Clim 27:5724–5745. https://doi.org/10.1175/jcli-d-13-00399.1

Dee DP, Uppala SM, Simmons AJ, Berrisford P, Poli P, Kobayashi S, Andrae U, Balmaseda MA, Balsamo G, Bauer P, Bechtold P, Beljaars AC, Van de Berg L, Bidlot J, Bormann N, Delsol C, Dragani R, Fuentes M, Geer AJ, Haimberger L, Healy SB, Hersbach H, Hólm EV, Isaksen L, Kållberg P, Köhler M, Matricardi M, McNally AP, Monge-Sanz BM, Morcrette JJ, Park BK, Peubey C, De Rosnay P, Tavolato C, Thépaut JN, Vitart F (2011) The ERA-Interim re-analysis: configuration and performance of the data assimilation system. QJR Meteorol Soc 137:553–597

Dominguez C, Magaña V (2018) The role of tropical cyclones in precipitation over the tropical and subtropical North America. Front Earth Sci 6:19. https://doi.org/10.3389/feart.2018.00019

Done JM, Holland GJ, Bruyère CL, Leung LR, Suzuki-Parker A (2015) Modeling high-impact weather and climate: lessons from a tropical cyclone perspective. Clim Change 129:381. https://doi.org/10.1007/s10584-013-0954-6

Emanuel KA (1997) Some aspects of hurricane inner-corner dynamics and energetic. J Atmos Sci 54:1014–1026. https://doi.org/10.1175/1520-0469(1997)054%3c1014:saohic%3e2.0.co;2

Enfield DB, Mestas-Nunez AM, Trimble PJ (2001) The Atlantic Multidecadal Oscillation and its relationship to rainfall and river flows in the continental U.S. Geophys Res Lett 28:2077–2080

Goldenberg SB, Landsea C, Mestas-Nuñez AM, Gray W (2001) The recent increase in Atlantic Hurricane activity: causes and implications. Science 293:474–479

Han J, Pan HL (2011) Revision of convection and vertical diffusion schemes in the NCEP global forecast system. Weather Forecast 26:520–533

Hong S-Y, Dudhia J, Chen S-H (2004) A revised approach to ice-microphysical processes for the bulk parameterization of cloud and precipitation. Mon Weather Rev 132:103–120

Hong S-Y, Noh Y, Dudhia J (2006) A new vertical diffusion package with an explicit treatment of entrainment processes. Mon Weather Rev 134:2318–2341. https://doi.org/10.1175/mwr3199.1

Hsieh JS, Cook KH (2007) A study of the energetics of African easterly waves using regional climate model. J Atmos Sci 64:421–440

Janiga MA, Thorncroft CD (2016) The influence of African easterly waves on convection over tropical Africa and the east Atlantic. Mon Weather Rev 144:171–192

Janjic ZI (1994) The Step-Mountain Eta Coordinate Model: further developments of the convection, viscous sublayer, and turbulence closure schemes. Mon Weather Rev 122:927–945

Jiang H, Zipser EJ (2010) Contribution to the global precipitation from eight seasons of TRMM data: regional, seasonal and interannual variations. J Clim 23:1526–1543

Kain JS, Fritsch JM (1990) A one-dimensional entraining/detraining plume model and its application in convective parameterization. J Atmos Sci 47:2784–2802. https://doi.org/10.1175/1520-0469(1990)047%3c2784:aodepm%3e2.0.co;2

Kiladis G, Wheeler M, Haertel P, Straub K, Roundy P (2009) Convectively coupled equatorial waves. Rev Geophys 47:RG2003. https://doi.org/10.1029/2008rg000266

Kim J, Alexander M (2013) Tropical precipitation variability and convectively coupled equatorial waves on submonthly time-scales in reanalysis and TRMM. J Clim 26:3013–3030. https://doi.org/10.1175/jcli-d-12-00353.1

Klotzbach PJ, Barnston A, Bell G, Camargo SJ, Chan JCL, Lea A, Sauders M, Vitart F (2011) Seasonal forecasting of tropical cyclones. In: Guard C (ed) Global guide to tropical cyclone forecasting, 2nd edn. World Meteorological Organization, Geneva

Klotzbach PJ, Saunders MA, Bell GD, Blake ES (2017) North atlantic seasonal hurricane prediction. In: Wang SS, Yoon J, Funk CC, Gillies RR (eds) Climate extremes: patterns and mechanisms, *Geophys Monogr Series*, 1st edn. Wiley, New York. https://doi.org/10.1002/9781119068020.ch19

Landsea CW, Franklin JL (2013) Atlantic hurricane database uncertainty and presentation of a new database format. Mon Weather Rev 141:3576–3592

Lubis SW, Jacobi C (2015) The modulating influence of convectively coupled equatorial waves (CCEWs) on the variability of tropical precipitation. Int J Climatol 35:1465–1483. https://doi.org/10.1002/joc.4069

Magaña V, Vázquez JL, Pérez JL, Pérez JB (2003) Impact of El Niño on precipitation in Mexico. Geofis Int 42:313–330

Marengo JA, Nobre CA, Tomasella J, Oyama MD, Sampaio de Oliveira G, De Oliveira R, Camargo H, Alves LM, Brown IF (2008) The drought of Amazonia in 2005. J Clim 21(3):495–516

Mlawer EJ, Taubman SJ, Brown PD, Iacono MJ, Clough SA (1997) Radiative transfer for inhomogeneous atmospheres: RRTM, a validated correlated-k model for the longwave. J Geophys Res 102D:16663–16682

Pasch RJ, Avila LA, Jiing J-G (1998) Atlantic tropical systems of 1994 and 1995: a comparison of a quiet season to a near-record-breaking one. Mon Weather Rev 126:1106–1123

Powers JG, Klemp JB, Skamarock WC, Davis CA, Dudhia J, Gill DO, Coen JL, Gochis DJ, Ahmadov R, Peckham SE, Grell GA, Michalakes J, Trahan S, Benjamin SG, Alexander CR, Dimego GJ, Wang W, Schwartz CS, Romine GS, Liu Z, Snyder C, Chen F, Barlage MJ, Yu W, Duda MG (2017) The weather research and forecasting model: overview, system efforts, and future directions. Bull Am Meteorol Soc 98:1717–1737. https://doi.org/10.1175/bams-d-15-00308.1

Reynolds RW, Smith TM, Liu C, Chelton DB, Casey KS, Schlax MG (2007) Daily high-resolution-blended analyses for sea surface temperature. J Clim 20:5473–5496

Schreck CJ, Molinari J, Anantha A (2012) A global view of equatorial waves and tropical cyclogenesis. Mon Weather Rev 140:774–788

Serra YL, Kiladis GN, Cronin MF (2008) Horizontal and vertical structure of easterly waves in the Pacific ITCZ. J Atmos Sci 65:1266–1284

Serra YL, Kiladis GN, Hodges KI (2010) Tracking and mean structure of easterly waves over the intra-Americas sea. J Clim 23:4823–4840

Thompson G, Rasmussen RM, Manning K (2004) Explicit forecasts of winter precipitation using an improved bulk microphysics scheme. Part I: description and sensitivity analysis. Mon Weather Rev 132:519–542

Thorncroft C, Hodges K (2001) African easterly wave variability and its relationship to Atlantic tropical cyclone activity. J Clim 14:1166–1179

Tiedtke M (1989) A comprehensive mass flux scheme for cumulus parameterization in largescale models. Mon Weather Rev 117:1779–1800

Vitart F (2017) Madden-Julian Oscillation prediction and teleconnections in the S2S database. QJR Meteorol Soc 143:2210–2220. https://doi.org/10.1002/qj.3079

Walter AP, Cifelli R, Boccippio DJ, Rutledge SA, Fairall C (2003) Convection and easterly wave structures observed in the eastern pacific warm pool during EPIC-2001. J Atmos Sci 60:1754–1773

Wang C, Enfield DB (2003) A further study of the tropical western hemisphere warm pool. J Clim 16:1476–1493